



HAL
open science

Patching up dipoles: Can dipolar particles be viewed as patchy colloids?

Jose Maria Tavares, Paulo Ivo Teixeira

► **To cite this version:**

Jose Maria Tavares, Paulo Ivo Teixeira. Patching up dipoles: Can dipolar particles be viewed as patchy colloids?. *Molecular Physics*, 2011, pp.1. 10.1080/00268976.2010.544266 . hal-00686163

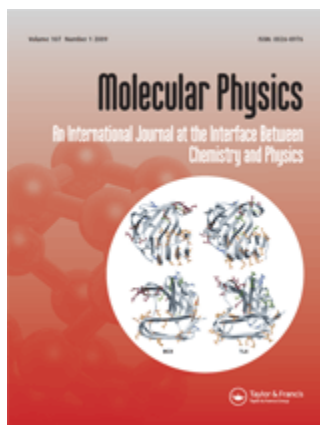
HAL Id: hal-00686163

<https://hal.science/hal-00686163>

Submitted on 8 Apr 2012

HAL is a multi-disciplinary open access archive for the deposit and dissemination of scientific research documents, whether they are published or not. The documents may come from teaching and research institutions in France or abroad, or from public or private research centers.

L'archive ouverte pluridisciplinaire **HAL**, est destinée au dépôt et à la diffusion de documents scientifiques de niveau recherche, publiés ou non, émanant des établissements d'enseignement et de recherche français ou étrangers, des laboratoires publics ou privés.



Patching up dipoles: Can dipolar particles be viewed as patchy colloids?

Journal:	<i>Molecular Physics</i>
Manuscript ID:	TMPH-2010-0423.R1
Manuscript Type:	Special Issue paper - In honour of Bob Evans
Date Submitted by the Author:	18-Nov-2010
Complete List of Authors:	Tavares, Jose; Instituto Superior de Engenharia de Lisboa, Centro de Fisica Teorica e Computacional Teixeira, Paulo; Instituto Superior de Engenharia de Lisboa, Centro de Fisica Teorica e Computacional
Keywords:	Liquid-vapour transition, Self-assembly, Magnetic fluids
<p>Note: The following files were submitted by the author for peer review, but cannot be converted to PDF. You must view these files (e.g. movies) online.</p> <p>source files.zip</p>	

SCHOLARONE™
Manuscripts

Can dipolar particles be viewed as patchy colloids?

J. M. Tavares^{1,2} and P. I. C. Teixeira^{1,2}¹*Instituto Superior de Engenharia de Lisboa**Rua Conselheiro Emídio Navarro 1, P-1950-062 Lisbon, Portugal*²*Centro de Física Teórica e Computacional da Universidade de Lisboa**Avenida Professor Gama Pinto 2, P-1649-003 Lisbon, Portugal*

(Dated: 17 November 2010)

Abstract

We investigate whether the liquid-vapour phase transition of strongly dipolar fluids can be understood using a model of patchy colloids. These consist of hard spherical particles with three short-ranged attractive sites (patches) on their surfaces. Two of the patches are of type A and one is of type B . Patches A on a particle may bond either to a patch A or to a patch B on another particle. Formation of an AA (AB) bond lowers the energy by ϵ_{AA} (ϵ_{AB}). In the limit $\epsilon_{AB}/\epsilon_{AA} \ll 1$, this patchy model exhibits condensation driven by AB -bonds (Y-junctions). Y-junctions are also present in low-density, strongly dipolar fluids, and have been conjectured to play a key role in determining their critical behaviour. We map the dipolar Yukawa hard-sphere (DYHS) fluid onto this $2A + 1B$ patchy model by requiring that the latter reproduce the correct DYHS critical point as a function of the isotropic interaction strength ϵ_Y . This is achieved for sensible values of ϵ_{AB} and the bond volumes. Results for the internal energy and the particle coordination number are in qualitative agreement with simulations of DYHSs. Finally, by taking the limit $\epsilon_Y \rightarrow 0$, we arrive at a new estimate for the critical point of the dipolar hard-sphere fluid, which agrees with extrapolations from simulation.

PACS numbers: 64.70.F-, 64.75.Yz, 47.65.Cb

I. INTRODUCTION

1
2 Even after some forty years of efforts we still do not know whether dipolar forces alone
3 suffice to condense a vapour into a liquid. We shall not, of course, attempt to solve this
4 difficult problem here. Rather, we will show how some of our results for a different model
5 system, where liquid-vapour coexistence is also elusive, may be relevant to the criticality of
6 dipolar fluids. But first we give a brief review of the current state of our knowledge.
7
8

9
10 In the classic Van der Waals picture of phase transitions, simple fluids interact via
11 isotropic intermolecular potentials that comprise a short-ranged repulsion and a longer-
12 ranged attraction. Condensation is then driven by the free energy balance between the
13 high-entropy vapour phase (where attraction dominates) and the low-energy liquid phase.
14 (where repulsion prevails).
15
16

17
18 Most molecular species, however, exhibit permanent dipole moments. The simplest model
19 of a dipolar fluid is the dipolar hard sphere (DHS) fluid, which consists of hard spheres of
20 diameter σ , having at their centre a dipole moment of strength μ . The dipole-dipole
21 interaction is strongly anisotropic and long-ranged, hence notoriously difficult to treat theo-
22 retically. For this reason, a number of authors [1–5] have sought to derive isotropic *effective*
23 interaction potentials that nevertheless capture the essentials of the true dipolar fluid, for
24 the purpose of easier computation of its phase behaviour. In all cases, the leading term
25 of this effective potential is attractive and has the same distance dependence as, e.g., the
26 long-range part of the Lennard-Jones (LJ) potential. de Gennes and Pincus [6] conjectured
27 that the phase diagram of DHSs should be similar to that of a Van der Waals fluid, with
28 vapour, liquid and solid phases.
29
30

31
32 Surprisingly, however, numerical simulations of DHS [7] and also of Stockmayer fluids [8]
33 have revealed that the anisotropy of the dipolar potential promotes the formation of self-
34 assembled aggregates (chains, rings and more complex clusters) if the dipolar interaction
35 strength is of the order of the thermal energy. This is in sharp contrast with the isotropic
36 compact clusters observed in simple fluids. Moreover, unlike in simple fluids the pair cor-
37 relation function of DHS is strongly peaked at contact and the internal energy is nearly
38 independent of the density [9]. It is at present unclear whether strong association pre-empts
39 condensation, or any other kind of fluid-fluid phase separation, as failure to observe it may
40 be an artifact of the simulation techniques [10–13]. New methods are needed to allow a re-
41
42
43
44
45
46
47
48
49
50
51
52
53
54
55
56
57
58
59
60

assessment of the dipolar and related condensation problems in the light of recent theoretical results [14].

Thus dipolar particles may or may not condense, but they certainly associate. The simplest theories of association as applied to this system [15–19] assume that the only effect of the strongly anisotropic interparticle interaction is to drive cluster formation. Consequently, the fluid is described as an ideal mixture of self-assembling clusters, failing to exhibit any phase transitions unless direct or indirect interactions between the clusters are added. Nevertheless, these theories reproduce well the slow variation of the internal energy with the density and cluster size (or mass) distribution. Alternative treatments of the competition between phase separation and association in the Stockmayer and DHS fluids include variants of the Flory-Huggins (FH) model of equilibrium polymerisation [20, 21] and a thermodynamic perturbation theory for associating fluids [22, 23]. The former rely on casting the free energy of the Stockmayer fluid in FH form; the latter includes a contribution from association to the free energy, but does not distinguish between chaining and branching, the two types of self-assembly that appear to influence the phase behaviour of dipolar fluids.

A different approach to the phase behaviour of the dipolar fluid was proposed in [24]. Following the results for the structure suggested by simulations (long chains that may form branches, see, e.g. [18]), it was assumed that the dipolar fluid at low densities and temperatures can be described as a perturbation of a ground state that consists of infinitely long chains. This perturbation consists of the appearance of two types of thermally excited defects: end defects, which correspond to the formation of shorter chains, and Y-junction defects, which correspond to the merging of three chains. Chain ends and junctions carry energy penalties ϵ_e and ϵ_j , respectively. The entropic gain of defect forming is related to the lattice model from which the free energy was derived [25]. It was shown that a critical point would exist only if the energy cost of forming a junction is small enough, $\epsilon_j < \frac{\epsilon_e}{3}$. When such a critical point exists, phase coexistence is obtained between a low-density gas of short chains (i.e., rich in end defects) and a high-density networked liquid (i.e., rich in Y-junctions). More strikingly, it was found that the phase diagram displays a *pinched*, or reentrant, behaviour: as temperature is decreased, the densities of the coexisting liquid and vapour phases become more similar, rather than more different, as is the norm in most fluids. This model thus introduces a new perspective on association in dipolar fluids: the anisotropy of the dipolar potential promotes competition between chaining and branching,

1 which determines the peculiar phase behaviour of DHSs. Safran's model can be quantita-
2 tively related to the dipolar fluid by expressing the two energy scales ϵ_j , ϵ_e , in terms of the
3 dipole moment. The shortcomings of this description of the DHS fluid are: (i) the difficulty
4 of relating ϵ_j and the dipole moment; (ii) its origin in a lattice model, which hinders quan-
5 titative comparion with continuous models like DHSs; and (iii) the asymptotic character of
6 its thermodynamics, which is only valid at extremely low densities and temperatures.
7
8

9 In recent work [26], we have established an analogy between Thusty and Safran's (TS)
10 model [24] and patchy particles with three bonding sites (patches), two of type A and one of
11 type B . In this model, henceforth denoted $2A + 1B$ model, particles can bind to each other
12 through their patches, thereby forming AA bonds that lower the energy by ϵ_{AA} , and AB
13 bonds that lower the energy by ϵ_{AB} . If $\epsilon_{AA} > 2\epsilon_{AB}$, the ground state consists of long chains of
14 particles connected by AA bonds. Two end defects are created when a long chain breaks into
15 two, with an energy cost of ϵ_{AA} . A Y-junction is formed when, after breaking a long chain
16 into two, one of the ends (a non-bonded A patch) bonds to an interior particle of another
17 chain (to a non-bonded B patch), creating a AB bond. The energy cost of this Y-junction
18 is thus $-\epsilon_{AB} + \epsilon_{AA}/2$. Moreover, it was also shown that Wertheim's first order perturbation
19 theory [27–30], as applied to the patchy model predicts the same phase behaviour as TS:
20 a critical point can only exist if $\epsilon_{AB} > \epsilon_{AA}/3$ (which is equivalent to $\epsilon_j > \epsilon_e/3$ in the TS
21 model); coexistence, when present, is between a low-density phase with few AA and AB
22 bonds, and a high-density phase rich in AB and AA bonds; and *pinching* is also observed
23 [31].
24
25
26
27
28
29
30
31
32
33
34
35
36

37 Despite the similiraties between the TS model and the patchy model, there are advan-
38 tages in using the latter. These come from the fact that the patchy model, combined with
39 Wertheim's perturbation theory, yields a thermodynamics that is able to describe a fluid.
40 In fact, TS relies on a lattice model and, in its thermodynamic description, the entropy of
41 the ends and junctions is solely related to the properties of the underlying lattice [25]. By
42 contrast, the entropy of the bonded patches is related to their size and to the properties
43 of the reference system [26, 32]. Therefore, when comparing both models with simulation
44 results, better agreement is expected for the patchy model.
45
46
47
48
49
50

51 Our purpose is to provide a simple analogy between the $2A + 1B$ model and DHSs. This
52 analogy will be quantitatively tested by comparing our theoretical results for the thermo-
53 dynamics and the structure of the patchy model, with those of simulations of the dipolar
54
55
56
57
58
59
60

Yukawa hard-sphere (DYHS) fluid [13, 23], for decreasing values of the isotropic Yukawa interaction strength.

This paper is organized as follows: in section II we detail the analogy between the patchy model and the DYHS (II A), and use Wertheim's perturbation theory to derive the thermodynamics (II B). Results for the critical parameters, phase diagrams, internal energy and particle coordination numbers are presented and discussed in section III. Finally in section IV we conclude and highlight further directions for research.

II. THEORY

A. Analogy between DYHSs and patchy particles

The DYHS fluid studied in [13, 23] consists of hard spheres (HSs) of diameter σ with a central point dipole of strength μ and interacting through a potential that comprises two contributions: the anisotropic dipole-dipole interaction and a Yukawa isotropic attraction of energy scale ϵ_Y and decay parameter z (we have set $z = 1.8$ for consistency with [13, 23]).

The $2A + 1B$ model of patchy particles will then consist of HSs of diameter σ , which attract isotropically through the same Yukawa potential as the DYHS fluid, but where the central dipole has been replaced by two patches of type A and one patch of type B , placed on the HS surface [26]. These patches may form AA and AB bonds, which lower the energy by ϵ_{AA} and ϵ_{AB} , respectively. To proceed with this analogy, ϵ_{AA} and ϵ_{AB} must be related to the dipolar energy scale μ^2/σ^3 . A sketch of this analogy is given in figure 1.

When $\epsilon_{AA} > \epsilon_{AB}/2$ (and $\epsilon_Y = 0$) the ground state of the $2A+1B$ patchy particles consists of long chains connected by AA bonds. Likewise, the ground state of DHSs consists of long chains (or rings) of particles aligned head to tail. Because the absolute minimum of the DHS pair potential (the energy of two dipolar spheres at contact and aligned head to tail) is $2\mu^2/\sigma^3$, we shall take

$$\epsilon_{AA} = 2\mu^2/\sigma^3. \quad (1)$$

This first relation between the DHS and $2A + 1B$ models is therefore obtained by matching their ground states.

The relation between ϵ_{AB} and the dipolar energy is established by considering branched Y-shaped arrangements (see figure 1b) containing N particles. It is this structure that,

together with the breakup of short chains, is expected to appear as a low-energy, thermally-excited perturbation of the ground state of infinite chains [24]. A Y-shaped arrangement of N DHSs that results from bringing together the ends of three chains of aligned dipoles (see figure 1b) has energy $-2(N-3)\mu^2/\sigma^3 - u_3\mu^2/\sigma^3$, where $-u_3\mu^2/\sigma^3$ is the dipolar interaction energy between the three dipoles that make up the junction. On the other hand, the Y-shaped arrangement of N patchy particles that results from bonding an A patch at a chain end with a B patch on an interior particle of another chain, has energy $-(N-2)\epsilon_{AA} - \epsilon_{AB}$. Matching these two results and using equation (1), we obtain

$$\epsilon_{AB} = (u_3 - 2)\mu^2/\sigma^3. \quad (2)$$

u_3 can be evaluated by considering three DHSs in contact (see figure 2). The configurations depicted show that a simple approximation for u_3 should be avoided. In fact, both configurations seem reasonable for Y-arrangements of dipoles: (a) results from slightly bending one chain and attaching another chain at the bend; (b) is a highly symmetric (ring-like) configuration that corresponds to the lowest possible energy. Choosing (a) or (b) has completely different consequences for the phase behaviour [26, 33]: (a) corresponds to $\epsilon_{AB}/\epsilon_{AA} \approx 0.105$ (i.e., $\epsilon_{AB}/\epsilon_{AA} < 1/3$) and thus to the absence of a critical point, whereas (b) corresponds to $\epsilon_{AB}/\epsilon_{AA} = 0.875$ (i.e., $\epsilon_{AB}/\epsilon_{AA} > 1/2$) and thus to the existence of a critical point that is not of the TS type, since the ground state is not a gas of long chains [31]. In order to avoid this somewhat arbitrary (and possibly biased) choice, we will let u_3 (or, equivalently, ϵ_{AB}) be a free parameter of the patchy model, and determine it by fitting the DYHS thermodynamics as determined by simulations [13] to that of our $2A + 1B$ model. Notice that this apparent shortcoming has one obvious advantage: we cannot know in advance whether the DHS fluid will exhibit a critical point. This conclusion will depend on the value obtained for ϵ_{AB} , which is determined not only by the analogy we propose, but also by the simulation results.

The bonding of A and B patches is characterised not only by two energy scales, but also by the bond volumes, v_{AA} and v_{AB} , [26, 32], which are related to the patch sizes. We will let these two volumes be free parameters of the patchy model, and they will also be determined by fitting the thermodynamics of the DYHS fluid to that of $2A + 1B$ patchy particles.

B. Free energy of the $2A + 1B$ patchy model

The free energy per particle f of the $2A + 1B$ patchy model with an additional Yukawa attracton will be approximated by:

$$\beta f = \beta f_{HS} + \beta f_b + \beta f_Y, \quad (3)$$

where $\beta \equiv 1/(k_B T)$, T is the temperature, k_B is the Boltzmann constant, f_{HS} is the HS contribution (which we approximate by the Carnahan-Starling CS expression [34]), f_b is the bonding contribution due to the patches, and f_Y is the Yukawa contribution.

For HSs with two A and one B patches, Wertheim's theory [27, 28, 36] gives the following expression for the bonding contribution to the free energy [26, 35]:

$$\beta f_b = 2 \ln X_A + \ln X_B - X_A - \frac{X_B}{2} + \frac{3}{2}, \quad (4)$$

where X_α is the probability of having a patch of type α *not* bonded. The variables X_α are related to the density and temperature through the laws of mass action that are derived by treating bond formation as a chemical reaction [27, 28, 36]. For the case where only AA and AB bonds can form, these are [26, 35],

$$X_A + 2\eta\Delta_{AA}X_A^2 + \eta\Delta_{AB}X_AX_B = 1, \quad (5)$$

$$X_B + 2\eta\Delta_{AB}X_AX_B = 1, \quad (6)$$

where $\eta \equiv (N/V)v_s$ is the packing fraction, and

$$\Delta_{\alpha\beta} = \frac{1}{v_s} \int_{v_{\alpha\beta}} g_{ref}(\mathbf{r}) [\exp(\beta\epsilon_{\alpha\beta}) - 1] d\mathbf{r}. \quad (7)$$

This integral is calculated over $v_{\alpha\beta}$, the volume of bond $\alpha\beta$, and g_{ref} is the pair correlation function (PCF) of the HS reference system. These equations yield the probability $p_\alpha = 1 - X_\alpha$ that a site of type α is bonded, as a function of density, temperature, and the interaction strengths. As we shall see, this enables us to calculate *structural* properties, in addition to thermodynamic properties.

The integral in equation (7) is evaluated by replacing the PCF by its value at contact in the CS approximation [34]:

$$g_{ref}(r) = g_{ref}(\sigma^+) = \frac{1 - \frac{\eta}{2}}{(1 - \eta)^3}. \quad (8)$$

This is expected to be reasonable provided that the typical size of the patches (and, consequently, that of the bonds) is $\ll \sigma$. Within this approximation, equation (7) becomes

$$\Delta_{\alpha\beta} = \frac{v_{\alpha\beta}}{v_s} [\exp(\beta\epsilon_{\alpha\beta}) - 1] \frac{1 - \frac{\eta}{2}}{(1 - \eta)^3}. \quad (9)$$

The contribution to the free energy coming from the Yukawa attraction, f_Y , will be given by a simple mean-field (MF) approximation, as used, e.g., in [36]:

$$\beta f_Y = -\frac{1}{2}\beta\eta \int \phi_Y(r_{12}) d\mathbf{r}_{12} = -2\pi\beta (z^{-1} + z^{-2}) \epsilon_Y \eta, \quad (10)$$

with, as in [12], $z = 1.8$. We expect equation (10) to become increasingly inaccurate as attractive Yukawa forces become dominant over dipolar forces and the density of the coexisting phases (as well as that of the critical point) increases. A slightly more sophisticated alternative consists in setting

$$\beta f_Y = -\beta B_2^Y \eta \approx \frac{2\pi}{3} \times 3.097 (\beta\epsilon_Y)^{1.0724} \eta \quad (11)$$

where B_2^Y is the second-virial coefficient of the HS Yukawa fluid, interpolated from the numerical results in [37] after subtracting the HS contribution (which is already contained in βf_{hs}). Below we shall assess the relative merits of equations (10) and (11); it turns out that there is very little difference between them in the ranges of parameters (ρ, T, ϵ_Y) of interest.

We are now in possession of a free energy, equation (3), which is a function of, besides (η, T), ϵ_{AB} , v_{AA} , v_{AB} (through equation (4)) and ϵ_Y (through equation (10) or equation (11)). We shall first derive the formal expressions for the critical density and temperature, and then search for the values of ϵ_{AB} , v_{AA} and v_{AB} that best reproduce the critical densities and temperatures found in the DYHS simulations of [12] for several values of ϵ_Y . Once these parameters are known, all thermodynamic quantities of interest can be calculated, as well as some structural properties.

III. RESULTS

We introduce reduced units defined as usual: reduced temperature $T^* = k_B T \sigma^3 / \mu^2$; reduced Yukawa energy parameter $\epsilon_Y^* = \epsilon_Y \sigma^3 / \mu^2$, reduced dipolar interaction parameter $(\mu^*)^2 = \mu / (\epsilon_Y \sigma^3) = 1 / \epsilon_Y^*$; reduced number density $\rho^* = \rho \sigma^3$. This amounts to taking σ , the

HS diameter, as our unit of length, and σ^3/μ^2 as our unit of energy. Note that this choice of energy scale is neutral from the point of view of criticality, as AA bonds can only lead to chaining, and not phase coexistence, at any finite temperature. The DHS limit corresponds to $\epsilon_Y^* = 0$.

We started by estimating the model parameters ϵ_{AB} , v_{AA} and v_{AB} , by requiring that our $2A + B$ patchy model reproduce the critical temperatures and densities listed in Table 1 of [13], for a range of Yukawa interaction strengths. This was achieved using the least-squares routine LMDIF from MINPACK library, coupled with NETLIB routine HYBRD for solving the critical point equations, which yielded the parameters collected in table I. The quality of fits, as measured by their root mean square deviation, does not depend strongly on how many points we fit, or how we treat the attractive Yukawa term. Note that, for all fits, one has $\epsilon_{AB}/\epsilon_{AA} < 1/2$, i.e., results are consistent with the hypothesis that the ground state of the system is long chains. These results therefore indicate that competition between chaining and branching plays a prominent role in the phase behaviour. Note also that, for all fits but one, $\epsilon_{AB}/\epsilon_{AA} > 1/3$, which strongly suggests that there exists a critical point in the DHS limit. Consequently, we predict that the critical point of the DHS fluid (corresponding to $\epsilon_Y^* = 0$) will occur at $T_c^* \approx 0.14 - 0.16$, $\rho_c^* \approx 0.03 - 0.05$, which is in line with earlier estimates reviewed in [13]. In what follows we have used the set of parameters shown in bold, chosen on the basis of (i) simplicity of the MF treatment of attractions; (ii) sensible values for v_{AA} and v_{AB} . The other sets of parameters (except the very first one, for which $\epsilon_{AA}/\epsilon_{AB} < 1/3$) nevertheless yield very similar results. Finally, one apparent shortcoming of these fits is that the values of $v_{\alpha\beta}$ are larger than those usually adopted in patchy particle models (see, e.g., [33]), which must not violate Wertheim's theory assumption that no more than two particles connect at any given bond. Further work is needed to clarify if the bond volumes in table I satisfy this requirement.

In figure 3 we plot the reciprocal of the critical temperature in Yukawa units (figure 3a), the critical temperature (figure 3b) and the critical density (figure 3c). Agreement, which is in general quite good, deteriorates slightly as we go to larger ϵ_Y^* , i.e., as we approach the non-polar Yukawa limit. This is a consequence of the fact that we fitted only to the six data points with smallest ϵ_Y^* (see above), coupled with our rather simplistic treatment of Yukawa attractions at the MF level.

We found the phase diagram by equating the pressures and chemical potentials of the

coexisting liquid and vapour phases, together with the mass-action law equations (5) and (6) for the two phases. The resulting set of six coupled non-linear equations was solved numerically using NETLIB routine HYBRD. Results are shown in figure 4, for different values of the Yukawa interaction parameter ϵ_Y^* . As $\epsilon_Y^* \rightarrow 0$ and the DHS limit is approached, the phase diagram develops a ‘pinch’, or re-entrance, at low temperatures: the densities of the coexisting liquid and vapour phases become more similar, rather than more different, as is the norm in most fluids. This is a consequence of the fact that $1/3 \leq \epsilon_{AB} \leq 1/2$, and was previously observed in a Monte Carlo simulation of a variant of our patchy fluid with two A and nine B patches [31]. In the present model this pinching only appears at the smallest ϵ_Y , for which the chaining/branching competition dominates over the effect of isotropic interactions.

The change in internal energy as a function of density at $T^* = 0.15$ and $\epsilon_Y^* = 0.025$, can be seen in figure 5a (to be compared with figure 4 of [13]). Whereas the *total* energy decreases with density, in agreement with the classical picture of the liquid (higher-density) phase as low-energy and low-entropy, the patchy contribution saturates, thus reproducing a characteristic footprint of DHSs. The latter contribution actually equals the internal energy of the patchy fluid at the same density and temperature, since our theory treats bonding and Yukawa attractive interactions separately.

In figure 5b we plot several structural quantities at the critical point, in order to describe the evolution of the structure of the fluid when ϵ_Y^* is varied. For extremely small ϵ_Y^* (i.e., close to the DHS limit), $\approx 90\%$ of A patches and $\approx 15\%$ of B patches are bonded. The number of AA bonds per particle is very large, hence there must be many long chains, forming Y-junctions whenever a B patch is bonded. This scenario seems to hold up to $\epsilon_Y^* \approx 0.1$, with slightly shorter chains (a decreasing fraction of AA bonds) and a larger number of Y-junctions (an increasing fraction of AB bonds). However, for $\epsilon_Y^* > 0.1$ there is a dramatic change in the fluid structure at the critical point: the number n of chains becomes negligible (there is a sharp decrease in the fraction of AA bonds) and the number of AB bonds, although decreasing, is larger than the number of AA bonds. Since the critical temperature and the critical density are both increasing, AB bonds become favoured relative to AA bonds, because the associated entropy is larger on account of $v_{AB} \gg v_{AA}$. Nevertheless, the total number of bonds decreases strongly and the fluid becomes less and less associated as ϵ_Y^* increases, as expected. Therefore, above $\epsilon_Y^* \approx 0.1$ criticality is already determined by

the Yukawa attraction and not by the competition between chaining and branching. This result shows that, as already discussed in [13], the DHS limit obtained from any model that approaches it, must be taken with care, since dramatic changes in the structure and thermodynamics are expected.

Finally, in figure 6 we show the variation with density at $T^* = 0.15$ of the fractions of particles bonded to zero (n_0), one (n_1), two (n_2) or three (n_3) other particles, corresponding to, respectively, isolated particles, chain ends, particles inside chains, or Y-junctions. These quantities are calculated using the probabilities $p_A = 1 - X_A$ and $p_B = 1 - X_B$, and assuming that bonds are independent. As the density increases $n_0 + n_1$ decreases rather sharply whereas n_3 gently increases, implying that the lower-density (vapour) phase is richer in chain ends and unattached particles, whereas the higher-density (liquid) phase is richer in junctions. n_2 , on the other hand, first rises sharply, indicating that chains are increasing in length, then reaches a maximum at $\rho^* \sim 0.04$, and finally drops very slowly, with increasing ρ^* . This slow decrease of n_2 (together with the increase in n_3) is of entropic origin: AA bonds are turning into AB bonds because $v_{AB} \gg v_{AA}$. Except for the initial increase in n_2 , the qualitative trends are the same as in the nearest-neighbour histograms of figure 6 of [13]; note, however, that the results in the latter figure do not extend below $\rho^* = 0.025$, and that n_2 appears to be peaking around that value (see middle panel of figure 6 in [13]).

IV. CONCLUSIONS

We have been able to map the DYHS fluid onto a model of patchy colloids with three interaction sites, two of type A and one of type B , where B sites do not interact. This was achieved by requiring that this model reproduce the critical densities and temperatures found from simulation, for a range of values of the Yukawa interaction parameter ϵ_Y^* . Wertheim's association theory as applied to this model is able to reproduce the correct trends of the particle coordination number: on increasing the density at constant temperature, the fraction of particles with zero (isolated particles), one (chain ends) or two (inner particles in chains) nearest neighbours decreases, whereas that of particles with three or more nearest neighbours (junctions or particles inside compact clusters) increases. Moreover, we predict that the dipolar contribution to the internal DYHS energy should saturate at high densities, again in agreement with simulations.

1
2
3
4
5
6
7
8
9
10
11
12
13
14
15
16
17
18
19
20
21
22
23
24
25
26
27
28
29
30
31
32
33
34
35
36
37
38
39
40
41
42
43
44
45
46
47
48
49
50
51
52
53
54
55
56
57
58
59
60

A more interesting consequence of using the $2A+1B$ patchy model is that, if our mapping is valid, then the phase diagram of DYHSs should be reentrant, or ‘pinched’ in the $\epsilon_Y^* \rightarrow 0$ limit: for $T^* \lesssim (2/3)T_c^*$, the density difference between the coexisting liquid and vapour phases *decreases* as the temperature is further lowered. This is in stark contrast to the behaviour of most fluids, but has actually been confirmed by simulation of $2A+9B$ patchy colloids [31]. Observation of the same effect for actual DYHS would be a stringent test of our approach.

In future work we plan to apply our mapping to other models that, while remaining simple to simulate and study theoretically, converge to the DHS on varying some parameter, e.g., mixtures of polar and non-polar HSs in the limit of infinite dilution of the latter.

Acknowledgement

Financial support from the Foundation of the University of Lisbon and the Portuguese Foundation for Science and Technology (FCT) under Contracts nos. POCI/FIS/55592/2004, POCTI/ISFL/2/618 and PTDC/FIS/098254/2008, as well as through Pluriannual contracts with CFTC, is gratefully acknowledged.

-
- [1] W. H. Keesom, Phys. Z. **22**, 129 (1921).
[2] C. E. Woodward and S. Nordholm, Molec. Phys. **52** 973 (1984).
[3] J. M. Mercer, Molec. Phys. **69**, 625 (1990).
[4] P. Frodl and S. Dietrich, Phys. Rev. A **45**, 7330 (1992).
[5] A. P. Philipse and B. W. M. Kuipers, J. Phys.: Condens. Matter **22**, 325104 (2010).
[6] P. G. de Gennes and P. Pincus, Phys. Kondens. Mater. **11**, 189 (1970).
[7] J. J. Weis and D. Levesque, Phys. Rev. Lett. **71**, 2729 (1993).
[8] M. E. van Leeuwen and B. Smit, Phys. Rev. Lett. **71**, 3991 (1993).
[9] P. J. Camp, J. C. Shelley and G. N. Patey, Phys. Rev. Lett. **84**, 115 (2000).
[10] J. C. Shelley, G. N. Patey, D. Levesque and J. J. Weis, Phys. Rev. E **59**, 3065 (1999).
[11] S. C. McGrother and G. Jackson, Phys. Rev. Lett. **76**, 4183 (1996).
[12] G. Ganzenmüller and P. J. Camp, J. Chem. Phys. **126**, 191104 (2007).
[13] G. Ganzenmüller, G. N. Patey and P. J. Camp, Molec. Phys. **107**, 403 (2009).

- [14] G. Ganzenmüller and P. J. Camp, *J. Chem. Phys.* **127**, 1545044 (2007).
- [15] R. van Roij, *Phys. Rev. Lett.* **76**, 3348 (1996).
- [16] R. P. Sear, *Phys. Rev. Lett.* **76**, 2310 (1996).
- [17] M. A. Osipov, P. I. C. Teixeira and M. M. Telo da Gama, *Phys. Rev. E* **54**, 2597 (1996).
- [18] J. M. Tavares, J. J. Weis and M. M. Telo da Gama, *Phys. Rev. E* **59**, 4388 (1999).
- [19] K. Van Workum and J. F. Douglas, *Phys. Rev. E* **71**, 031502 (2005).
- [20] J. Dudowicz, K. F. Freed and J. F. Douglas, *Phys. Rev. Lett.* **92**, 045502 (2004).
- [21] R. Hentschke, J. Bartke and F. Pesth, *Phys. Rev. E* **75**, 011506 (2007).
- [22] Y. V. Kalyuzhnyi, I. A. Protsykevych and P. T. Cummings, *Europhys. Lett.* **80**, 56002 (2007).
- [23] Yu. V. Kalyuzhnyi, I. A. Protsykevych, G. Ganzenmüller and P. J. Camp, *Europhys. Lett.* **84**, 26001 (2008).
- [24] T. Tlusty and S. A. Safran, *Science* **290**, 1328 (2000).
- [25] A. G. Zilman and S. A. Safran, *Phys. Rev. E* **66**, 051107 (2002).
- [26] J. M. Tavares, P. I. C. Teixeira and M. M. Telo da Gama, *Phys. Rev. E* **80**, 021506 (2009).
- [27] M. S. Wertheim, *J. Stat. Phys.* **35**, 19 (1984).
- [28] M. S. Wertheim, *J. Stat. Phys.* **35**, 35 (1984).
- [29] M. S. Wertheim, *J. Stat. Phys.* **42**, 459 (1986).
- [30] M. S. Wertheim, *J. Stat. Phys.* **42**, 477 (1986).
- [31] J. Russo, J. M. Tavares, P. I. C. Teixeira, M. M. Telo da Gama and F. Sciortino (unpublished).
- [32] F. Sciortino, E. Bianchi, J. F. Douglas and P. Tartaglia, *J. Chem. Phys.* **126**, 194903 (2007)
- [33] J. M. Tavares, P. I. C. Teixeira, M. M. Telo da Gama and F. Sciortino, *J. Chem. Phys.* **132**, 234502 (2010).
- [34] N. F. Carnahan and K. E. Starling, *J. Chem. Phys.* **51**, 635 (1969).
- [35] J. M. Tavares, P. I. C. Teixeira and M. M. Telo da Gama, *Molec. Phys.* **107**, 453 (2009).
- [36] G. Jackson, W. G. Chapman and K. E. Gubbins, *Molec. Phys.* **65**, 1 (1988).
- [37] D. J. Naresh and J. K. Singh, *Fluid Phase Eq.* **285**, 36 (2009).

n	Yukawa	$\epsilon_{AB}/\epsilon_{AA}$	v_{AA}/σ^3	v_{AB}/σ^3	RMS deviation	T_c^* (DHS)	ρ_c^* (DHS)
8	eq. (10)	0.284805	0.00222266	0.459357	0.00691166	—	—
7	eq. (10)	0.347745	0.00234394	0.231612	0.00564450	0.142	0.033
6	eq. (10)	0.37328	0.00220629	0.173476	0.00565144	0.150	0.040
8.	eq. (11)	0.390595	0.00259764	0.145093	0.00697690	0.151	0.040
7.	eq. (11)	0.46689	0.00282981	0.0665826	0.00695441	0.162	0.049
6.	eq. (11)	0.46331	0.00247637	0.0668395	0.00657444	0.161	0.049

TABLE I: Fit parameters for the DYHS. n is the number of points from Table 1 in [13] included, starting at the lowest ϵ_Y^* . For each set we also give the estimates for the critical temperature and density of the DHS fluid (corresponding to $\epsilon_Y^* = 0$).

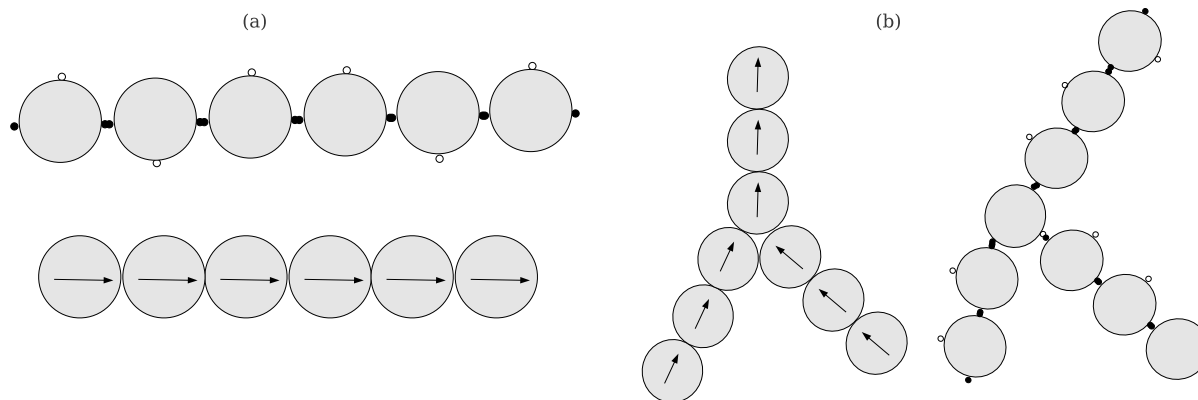


FIG. 1: Sketch of the mapping of the DHS fluid onto the $2A + 1B$ patchy model. The small black (white) circles represent patches of type A (B). (a) A linear chain of N DHSs, in contact and aligned head-to-tail, has energy $-2(N-1)\mu^2/\sigma^3$, whereas a row of N patchy particles has $N-1$ AA bonds and thus energy $-(N-1)\epsilon_{AA}$. (b) A Y -shaped arrangement, made up of N particles. In the DHS fluid this has energy $-2(N-3)\mu^2/\sigma^3 - u_3\mu^2/\sigma^3$ ($-u_3\mu^2/\sigma^3$ is the dipolar interaction energy of the three particles that have come together). In the $2A + 1B$ model, this forms when a free A patch A at a chain end bonds to a B patch on an interior particle of another chain; its energy is $-(N-2)\epsilon_{AA} - \epsilon_{AB}$.

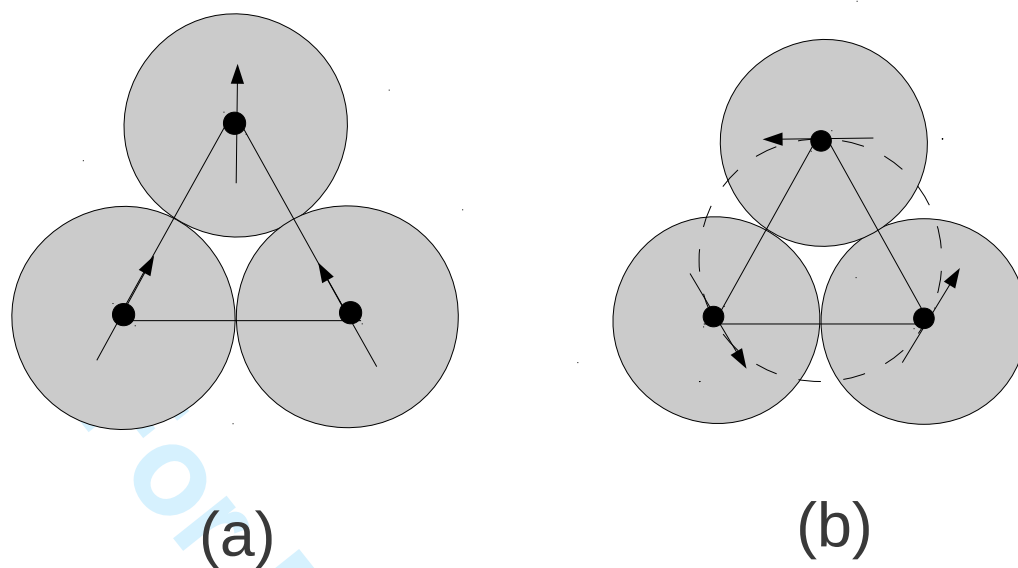


FIG. 2: Two examples of orientational configurations of three DHSs at contact. The dipolar energy of configuration (a) is $(-2\sqrt{3} + \frac{5}{4})\mu^2/\sigma^3 \approx -2.21\mu^2/\sigma^3$, and that of the ring configuration (b) is $-\frac{15}{4}\mu^2/\sigma^3$.

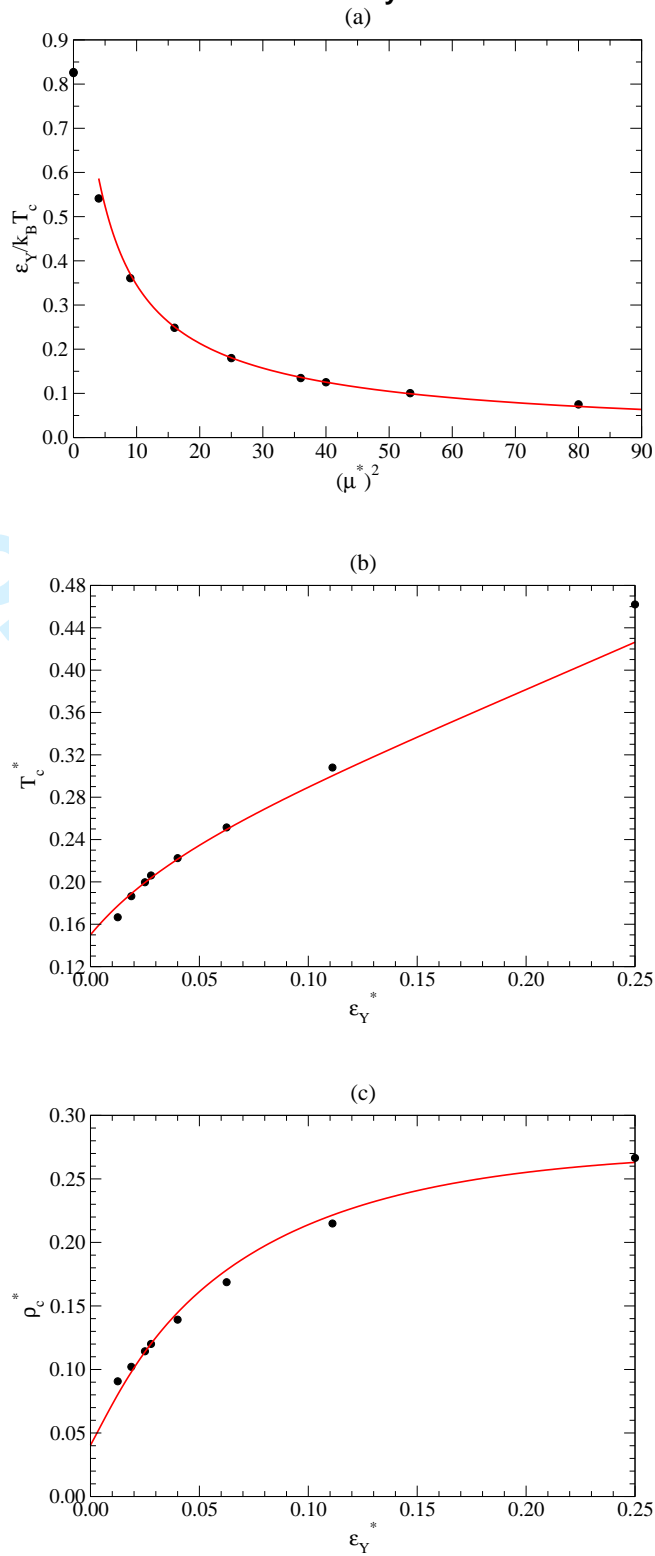


FIG. 3: (a) Reciprocal of the critical temperature in Yukawa units, $\epsilon_Y/k_B T_c$, vs the dipolar interaction parameter $(\mu^*)^2$; (b) critical temperature T_c^* and (c) critical density ρ_c^* , vs the Yukawa energy parameter ϵ_Y^* . The filled circles are simulation data from Table 1 in [13], the lines are fits from our theory, using the values boldfaced in table I for ϵ_{AB} , v_{AA} and v_{AB} . See the text for details.

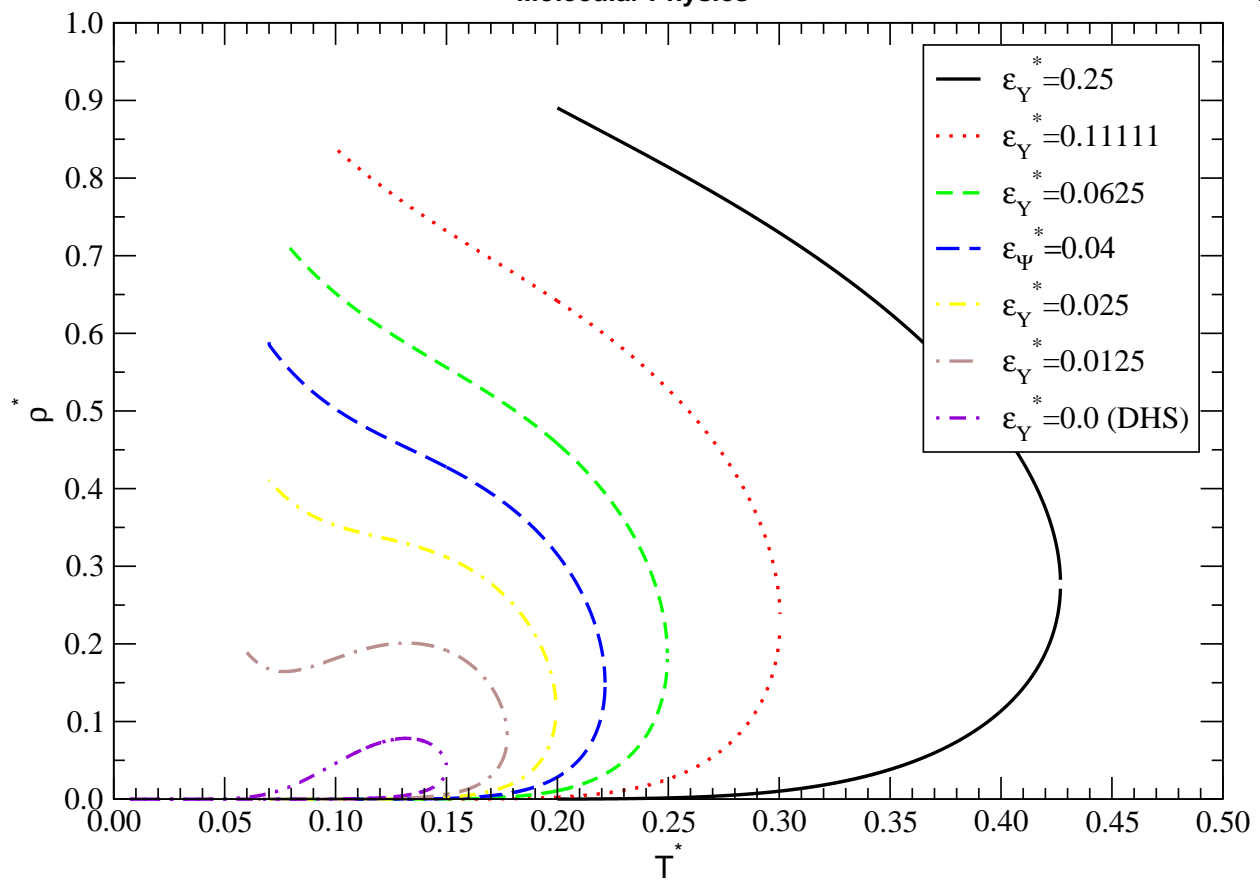


FIG. 4: Temperature-density phase diagram for different Yukawa interaction parameters ϵ_Y^* as shown, and ϵ_{AB} , v_{vAA} and v_{AB} as in figure 3. As $\epsilon_Y^* \rightarrow 0$ the diagrams ‘pinch’ (become re-entrant) at low temperatures, as seen in [31].

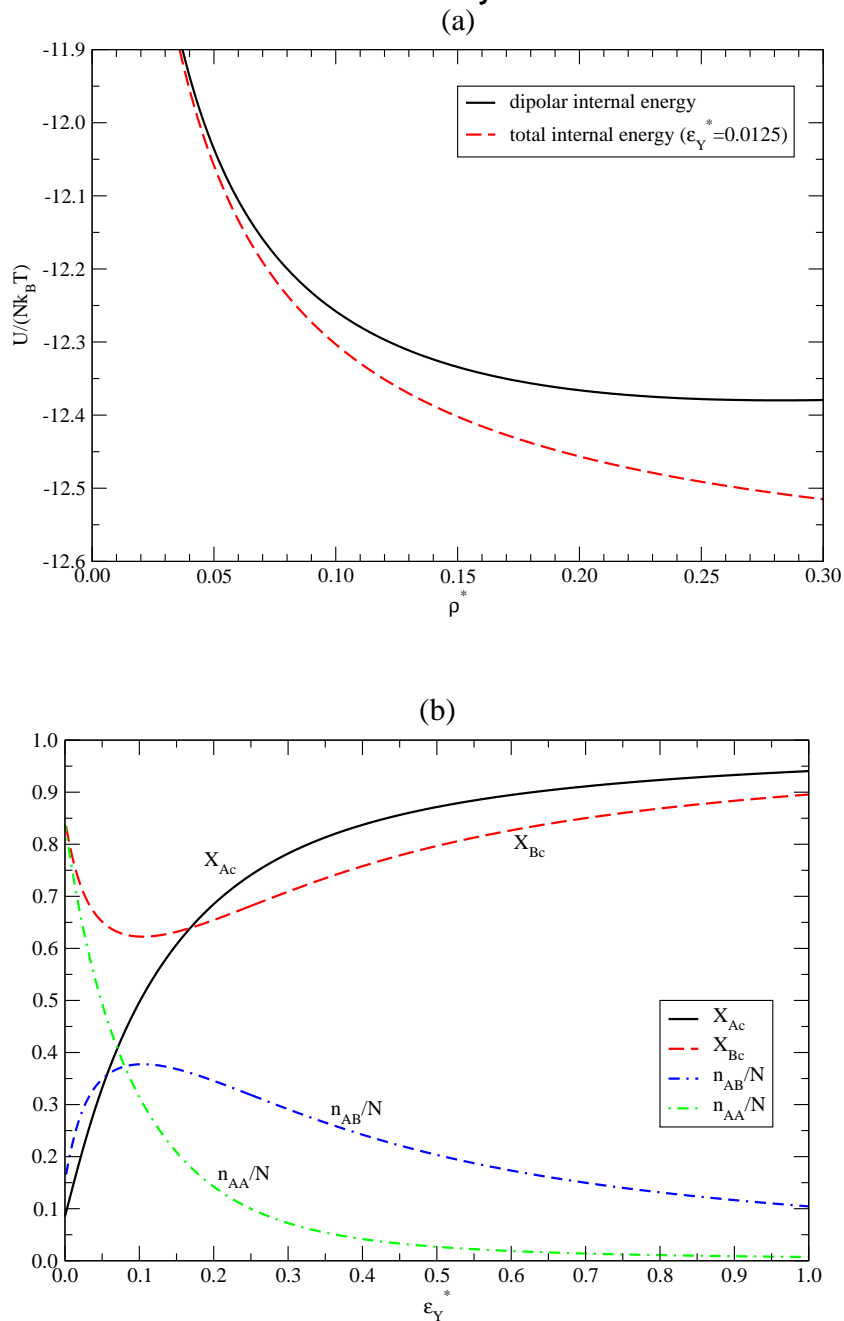


FIG. 5: (a) Total and dipolar potential energy per particle in units of $k_B T$ vs density ρ^* at a fixed temperature $T^* = 0.15$, for $\epsilon_Y^* = 0.0125$. The values of ϵ_{AB} , v_{AA} and v_{AB} are as in figure 3. As in figure 4 of [13], the dipolar energy saturates at higher densities. Notice that in our theory, the dipolar (i.e., patchy) contribution to the internal energy of the DYHS fluid is identical to the internal energy of the DHS fluid, since the Yukawa interaction does not affect bonding. (b) Degrees of non-association at the critical point, X_{Ac} and X_{Bc} : both approach 1 (the fully non-associated limit) as ϵ_Y^* grows and the fluid becomes less DHS-like and more Yukawa-like. We also plot the number of AA and AB bonds per particle at the critical point: $n_{AA}/N \equiv \frac{1+X_{Bc}}{2} - X_{Ac}$ and $n_{AB} \equiv 1 - X_{Bc}$.

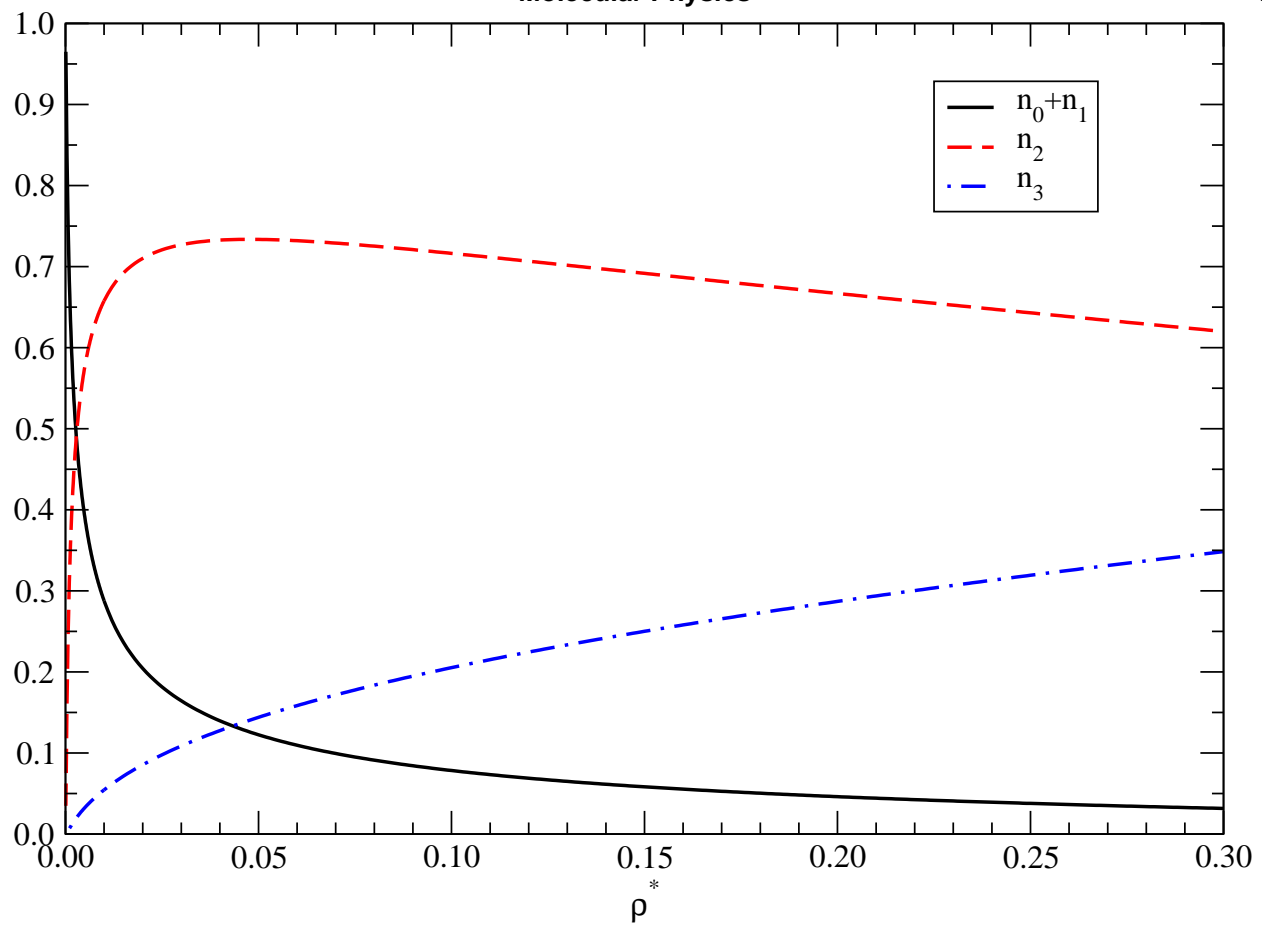


FIG. 6: Fractions of particles either not bonded or bonded to one other particle ($n_0 + n_1$), bonded to two other particles (n_2), or to three other particles (n_3), vs density at $T^* = 0.15$, for ϵ_{AB} , v_{AA} and v_{AB} as in figure 3. In our theory n_i do not depend on ϵ_Y^* . Compare with figure 6 of [13].